Current-carrying tribological performance of CrB$_2$/Cu composite coating prepared by laser cladding technology

Chen Zhang[1], Lei Jia[1,*] , Zhen-lin Lu[1], and Zhi-guo Xing[2,*]

[1] *School of Materials Science and Engineering, Xi`an University of Technology, Xi`an 710048, China*
[2] *National Key Lab for Remanufacturing, Academy of Armored Forces Engineering, Beijing 100072, China*

ABSTRACT

To repair and extend the service life of mobile-contact parts, laser cladding technology was applied to prepare CrB$_2$/Cu coating on Cu–Cr alloy substrate, which was simulated as actual servicing parts, and the current-carrying friction property, including that friction coefficient, wear rate as well as current-carrying efficiency were studied. Results show that most of the CrB$_2$ particles retain while some decompose into CrB$_x$ phases during the laser cladding process. With the increase of electric current, the average friction coefficient of CrB$_2$/Cu coating grows first followed by going down. In comparison to the CrB$_2$/Cu coating, the wear rate and average friction coefficient of QCr0.5 substrate always grow with increasing electric current values. When the current is 20A, the COF and wear rate of composite coating are about 0.737 and 1.37×10^{-4} mm^3/N•m, which are about 21% and 79% of that of QCr0.5 alloy, respectively, and the major wear mechanism of CrB$_2$/Cu coating is the adhesive wear. Moreover, the CrB$_2$/Cu composite coating has low friction coefficient, low wear rate and high current-carrying efficiency under high electric currents, as a consequence, the CrB$_2$/Cu coating has better current-carrying friction and wear performance under high current conditions.

1 Introduction

The electrical brush, sliding-electric contactor as well as conducting-electric joint are usually termed as the high-speed current-carrying mobile-contact parts, which need high conductivity and wear resistance for dealing with the server service conditions of advanced equipment [1, 2]. Pure copper and copper alloys are ideal raw materials for preparing such current-carrying mobile-contact parts due to their good thermal as well as electric conductivity. As the fast development of motor, railway, radar, etc. towards high power, high-speed, and high-accuracy [3, 4], it is essential for copper alloys to have higher performance. However, copper alloys, as the major high-speed current-carrying mobile-contact parts, always present poor wear resistance, especially when there is high electric current passing through the mobile-contact parts [5–7]. Hence, the current-carrying friction pairs are force-heat-electricity coupling system, namely, their

damage behavior includes mechanical damage, Joule heat effect, arc erosion as well as the coupling reaction of these factors. Consequently, the surface of mobile-contact parts is easy to be damaged.

Although the above damage always occurs on the surface with a depth of micrometer or even millimeter scale, the parts are always replaced by entirely new parts, which causes huge economic waste and environmental pollution [8] Recently, surface modification techniques have become more and more popular in many fields to repair or extend the life of surface failure parts, such as thermal spraying, electroplating process and ion implantation [8, 9]. The main drawback of thermal spraying technology is low bonding strength between the coating and substrate [10]. The electroplating technology will cause environmental pollution issue, which makes it difficult to meet the industry requirements [11]. The ion implantation technology will need the high cost of equipment and impair the electrical conductivity of material [9]. However, their limits can be overcome by laser cladding technology. The laser cladding method is one of the major surface modification techniques and owes many excellent advantages such as flexible operation, high efficiency, and degree of automation [12, 13]. In the laser cladding process, the powder material and a thin layer of substrate are melted together by the laser beam with high power, and thus forms a metallurgical bonding between the coating materials and substrate with low dilution [14].

Besides the repairing techniques, the special material system suitable for laser cladding process also needs to be studied [15]. Up to now, pure metal or alloying powder are the dominant raw materials for laser cladding coatings, but their wear resistance cannot compare with metal matrix composites, which is similar to the wear performance of metal matrix composites vs. the same matric metal [16, 17]. Especially for the Cu alloys used for preparing mobile-contact parts, the bad wear resistance needs urgent improvement. Transition metal boride has many excellent mechanical and physical properties such as good chemical stability, high melting and hardness. Compared with TiB_2 and ZrB_2 compounds, Cr-B compounds have lower electrical resistance, which makes it the first choice for reinforcing phase [18]. Among them, CrB_2 is the most stable compound and the melting point is 2200 °C, which is an ideal reinforcement for Cu matrix composite [19, 20], In our previous work, CrB_2/Cu composite coating was fabricated on Cu alloy substrate by laser cladding [21], which overcame the difficulty of Cu based coatings caused by its low absorption ratio to red laser and high thermal conductivity [22, 23]. However, the specific friction and wear behavior of such a composite coating with current remained unknown.

2 Methodology

2.1 Materials and pretreatment

QCr0.5 sheet of 50 × 50 × 10 mm was used as simulated failed surface of electrical contacting parts, since most of them are manufactured by using this kind of material. Firstly, the surface of sheet was sandblasted and rinsed in an ultrasonic water bath for 10 min to remove oxides on the surface. Then, the substrate sheet was soaked in black ink (carbon content of 10 wt.%) and then dried in an oven at 120 °C for 10 min, which can overcome the issue of the low absorption rate of the Cu substrate. In addition, spherical Cu powder (99.99% purity, particle size of 48–106 μm) and 3 vol.% CrB_2 (99.99% purity, particle size of 1–5 μm) powder were used as raw powder, as shown in Fig. 1. These two kinds of

Fig. 1 SEM morphology of raw **a** pure copper and **b** CrB_2 powder
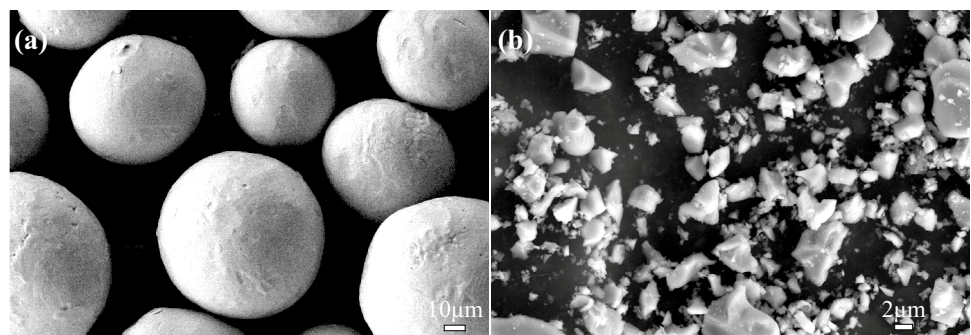
powder were mixed with ZrO_2 balls (ball-to-powder mass ratio of 1:3) by a rocking milling machine (RM-05-X, Seiwa Giken, Japan) at 50 Hz for 2 h, followed by drying in a vacuum oven at 50 °C for 6 h before laser cladding process.

2.2 Laser cladding process and parameters

The multi-layer laser cladding experiment was carried out on fiber laser equipment with a coaxial powder feeding system (ZKZM-2000, Zhongke Zhongmei Laser Technology Co., Ltd, Xi`an, China) and seven layers of cladding were repeated on the QCr0.5 substrate as shown in Fig. 2a. The scanning direction of the 1st, 3rd, 5th and 7th layer is parallel to the Y-axis, and that of the 2nd, 4th and 6th layer is parallel to the Y-axis, where the same processing parameters and a constant Z-axis lifting amount (0.33 mm) were used. The detailed parameters were laser beam power 1780 W, scanning speed 789 mm/min, defocus distance 8.3 mm and powder feed rate 2.8 g/min, which were optimized in our previous work [21]. The overlap ratio for adjacent track was 44% and the argon was used as a protective gas fixed at 4.2 L/min. The length (in X-axis) and width (in Y-axis) of each layer are around 45 mm and 25 mm, respectively. As a result, the total thickness of 7-layers coating was around 2.3 mm.

2.3 Test and characterizations

2.3.1 Current-carrying tribological test

The current-carrying tribological test was carried out on the multi-function friction tester (MS-M9000, Lanzhou Huahui Instrument Technology Co., Ltd., Lanzhou, China) with a pin-on-disk mode, as shown in Fig. 2b. The pin specimens (5 × 5 mm) were the composite coating that cut perpendicular from the laser cladding block by electrical discharge wire-cutting, while the counter disk was AISI 1080 steel. For comparison, QCr0.5 alloy was also machined into pin specimens with the same dimensions and underwent the current-carrying tribological test with the same parameters.

In the tribological experiment, the rotational speed and diameter were 500 r/min and 20 mm, the normal load was 15 N, the total time was 1 h (corresponding to sliding distance 1884 m), and the electric currents were 0, 5, 10, and 20 A, respectively, where three times were repeated for each current-carrying friction condition test to obtain average value. The wear mass loss of pin sample was measured by an electronic balance with an accuracy of 0.1 mg, and the volume wear rate (V_r) can be defined as follows [24]:

$$V_r = \frac{V_m}{F_n \times S} = \frac{M_m}{\rho \times F_n \times S},\tag{1}$$
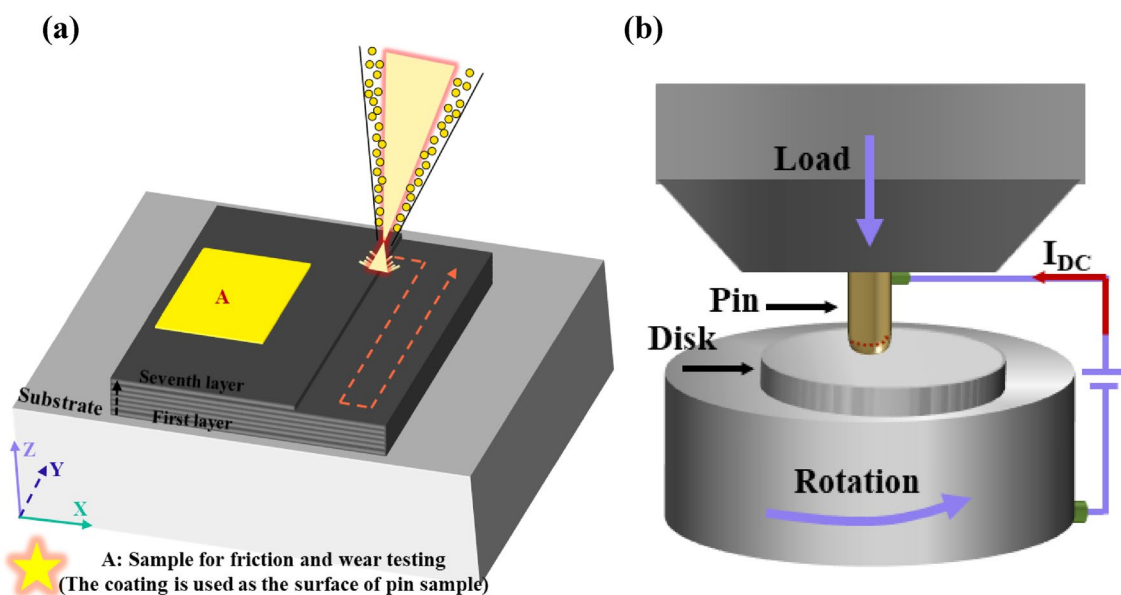
Fig. 2 Schematic diagram of **a** multi-layer laser cladding and **b** current-carrying wear test

where V_m, F_n, S, M_m and ρ are the volume loss (mm^3), normal load (N), sliding distance (m), mass loss and density of the pin sample, respectively.

The dynamic friction coefficient μ_i can be calculated as follows:

$$\mu_i = \frac{M_i}{F_i \times L}, \tag{2}$$

where M_i, F_i and L represent the friction torque recorded by the torque sensor of the machine, nominal load applied by weights, and the friction radius, respectively.

There will be some differences between the applied current provided by the power source and the measured value passed through the friction pairs, since the friction pair will be offline in the current-carrying friction test. Thus, current-passing efficiency (η_i) is an important parameter to describe the quality of current-carrying system, which is defined as follows [25]:

$$\eta_i = \frac{I_i}{I_s} \times 100\%, \tag{3}$$

where I_i represents the real current value passing through the friction pair in the test period (A), while I_s is the set current value of the constant current power source (A).

2.3.2 Materials characterizations

Microstructure of the laser-cladded composite coating in different regions was observed by optical microscopy (OM, Olympus) and scanning electronic microscopy (SEM, Merlin Compact) equipped with energy-dispersive spectroscopy (EDS, Oxford). Phase composition of the composite coating was detected by X-ray diffraction (XRD-7000, Shimadzu). Morphology of the worn surface was analyzed by SEM equipped with EDS.

3 Results and discussion

3.1 Microstructure

Figure 3 shows the results of microstructural characterizations on the top view surface of the laser-cladded CrB$_2$/Cu composite coating. It can be seen from the XRD patterns that, and coating mainly consists of Cu and CrB$_2$, besides a trace of CrB and Cr$_5$B$_3$ phases

(Fig. 3a). OM images show the whole morphology of the composite coating, where a large number of irregular particles distribute at the grain boundaries of the matrix (Fig. 3b, c). High magnification observation by SEM and the chemical composition analysis by EDS in Fig. 3d–f and d1–f1 show that some of the CrB$_2$ phase (dark particles) decomposes and forms new Cr-B intermetallics (white particles) around them, agreeing well with the results of XRD analysis. It is worth noting that the laser cladding process is a complex non-equilibrium process with a molten pool up to around 2400 °C [24, 26]. In such a case, the high-activity B atoms decompose from CrB$_2$ particles and can diffuse into Cu matrix and then form chromium borides with different stoichiometries (CrB$_x$). A similar phenomenon can also be found in other high-temperature surface treating technique [27, 28].

3.2 Current-carrying tribological properties

Figure 4 shows the dynamic coefficient of friction (COF) curves, the corresponding average COF values and the wear rate of the laser-cladded CrB$_2$/Cu composite coating as well as the contrast sample (QCr0.5 alloys) with different currents. With the increase of current, the average COF value of both composite coating and QCr0.5 alloy increase firstly, and the differences occur at 10A current, viz. the former one decreases but the latter one increases sharply, as seen in Fig. 4c. Compared with QCr0.5 material, the composite coating contains a certain number of CrB$_2$ particles which are exposed to the surface and the interaction force between the surface and counter face is increased thus causing the increasing friction coefficient when the current is below 10 A [29]. As the current subsequently exceeds 10 A, the temperature between the friction pairs rises. Because the thermal stability of CrB$_2$ particles would improve the hardness at elevated temperature, the surface of QCr0.5 is soften than CrB$_2$/Cu coating leading to heavy adhesive wear, namely, the coefficient of friction QCr0.5 is higher. On the whole, the COF values of composite coating is higher than that of QCr0.5 alloy under the current lower than 10A. Although a similar changing law of wear rate as COF can be found on these two materials with the change of current, the wear rate of the composite coating is always lower than that of QCr0.5 alloy, no matter how much current is applied (Fig. 4d). When a current of 20A is applied, the COF value and wear rate of composite coating are 0.737 and 1.37×10^{-4}
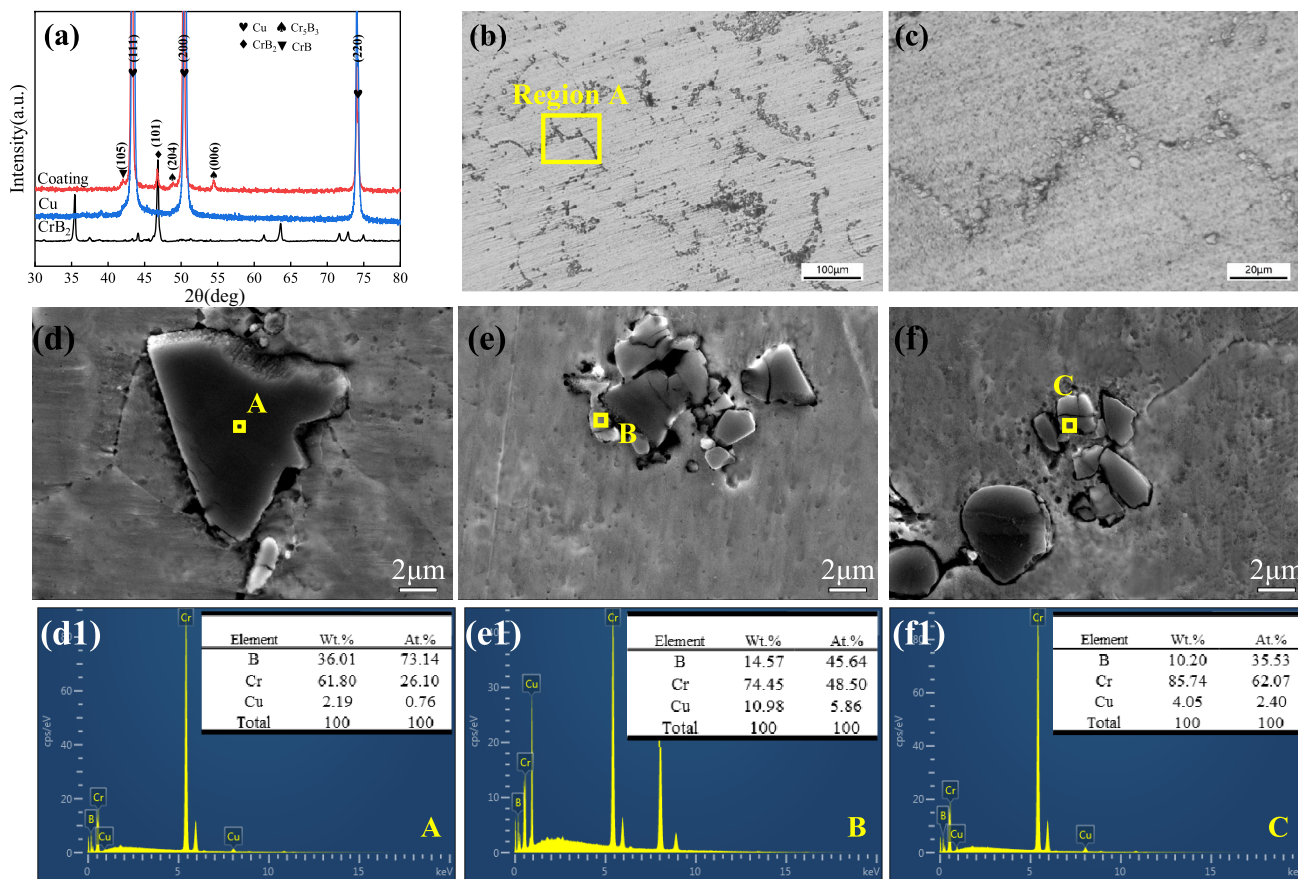
Fig. 3 Microstructural characterizations on the top view surface of laser-cladded CrB$_2$/Cu composite coating, **a** X-ray pattens of coating and raw materials, **b–c** optical images with different mag- nifications, **d–f** SEM images along with (d1-f1) EDS dot analyz- ing results on the marked areas, respectively

mm^3/N•m, which are about 21% and 79% of that of QCr0.5 alloy, respectively. Obviously, the composite coating has better wear resistance than the QCr0.5 alloy, and hence the friction and wear mechanism of them may change with the increase of applied current.

Figure 5 shows the current-passing efficiency (η) of CrB$_2$/Cu coating and QCr0.5 alloy during tribological tests with different current values. It is worth noting that the current-passing efficiency of both composite coating and QCr0.5 is nearly close to 100%, namely, the real current value passing through the friction pair is almost equal to the applied current value, suggest- ing that offline phenomenon is almost not appeared during tribological test. It is a fact that arc discharge is seldom seen during the experimental process, which means both the composite coating and QCr0.5 alloy have good arc resistance ability under the experimen- tal conditions. Comparatively speaking, although the η value of both composite coating and QCr0.5 alloy

decreases with the increase of loaded current, the declining speed of the former one is much smaller than the latter one. Obviously, the laser-cladded CrB$_2$/ Cu coating is more suitable than the QCr0.5 alloy that is usually used as the materials for manufacturing the real parts, when the working condition is high elec- trical current. However, the reason behind the differ- ent changing tendency between CrB$_2$/Cu coating and QCr0.5 alloy with the increase of applied current also needs to be clarified.

3.3 Friction and wear mechanism

To better understand the influence of current value on the tribological properties as well as the differences between CrB$_2$/Cu coating and QCr0.5 alloy, the mor- phologies of the worn surface under different current values were investigated and the results are shown in Fig. 6. It can be found from Fig. 6a that, when no
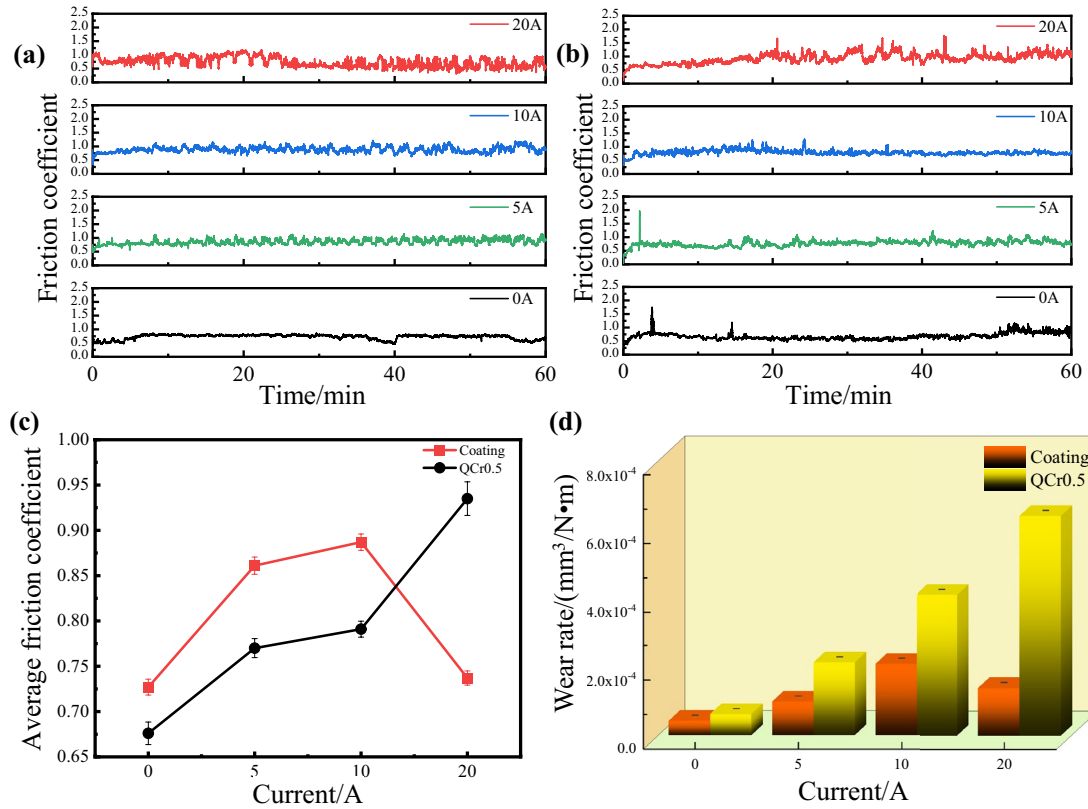
Fig. 4 Variations in the friction coefficients with time of **a** CrB₂/Cu composite coating and **b** QCr0.5, **c** average friction coefficient, **d** wear rate at different current value
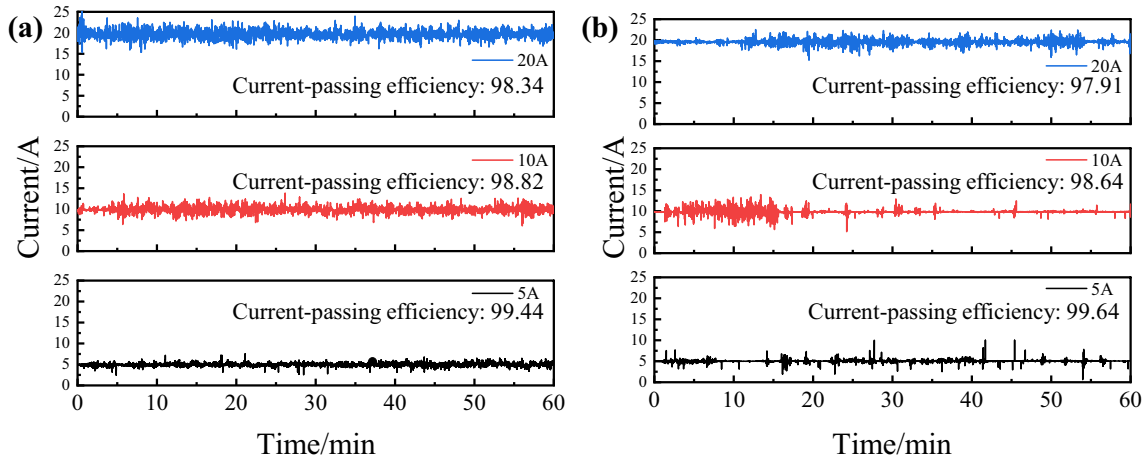
Fig. 5 Current-passing efficiency of **a** CrB₂/Cu coating and **b** QCr0.5 with different current values

current is applied, viz. only mechanical friction, there are obvious furrows, smooth plane by plastic deformation with some delamination, and cracks caused by fatigue, which agrees well with the microstructure

characters of the CrB₂/Cu composite coating. Herein, CrB₂ particles are responsible for the furrows, the plastic deformation of pure Cu matrix under load generates the smooth plane and adhesive delamination,

Fig. 6 SEM image of worn surface of **a**1-**a**4 CrB$_2$/Cu composite coating and **b**1-**b**4 QCr0.5 alloy after tribological tests with different values of current, where the subscript 1–4 means the current is 0A, 5A, 10A, and 20A, respectively
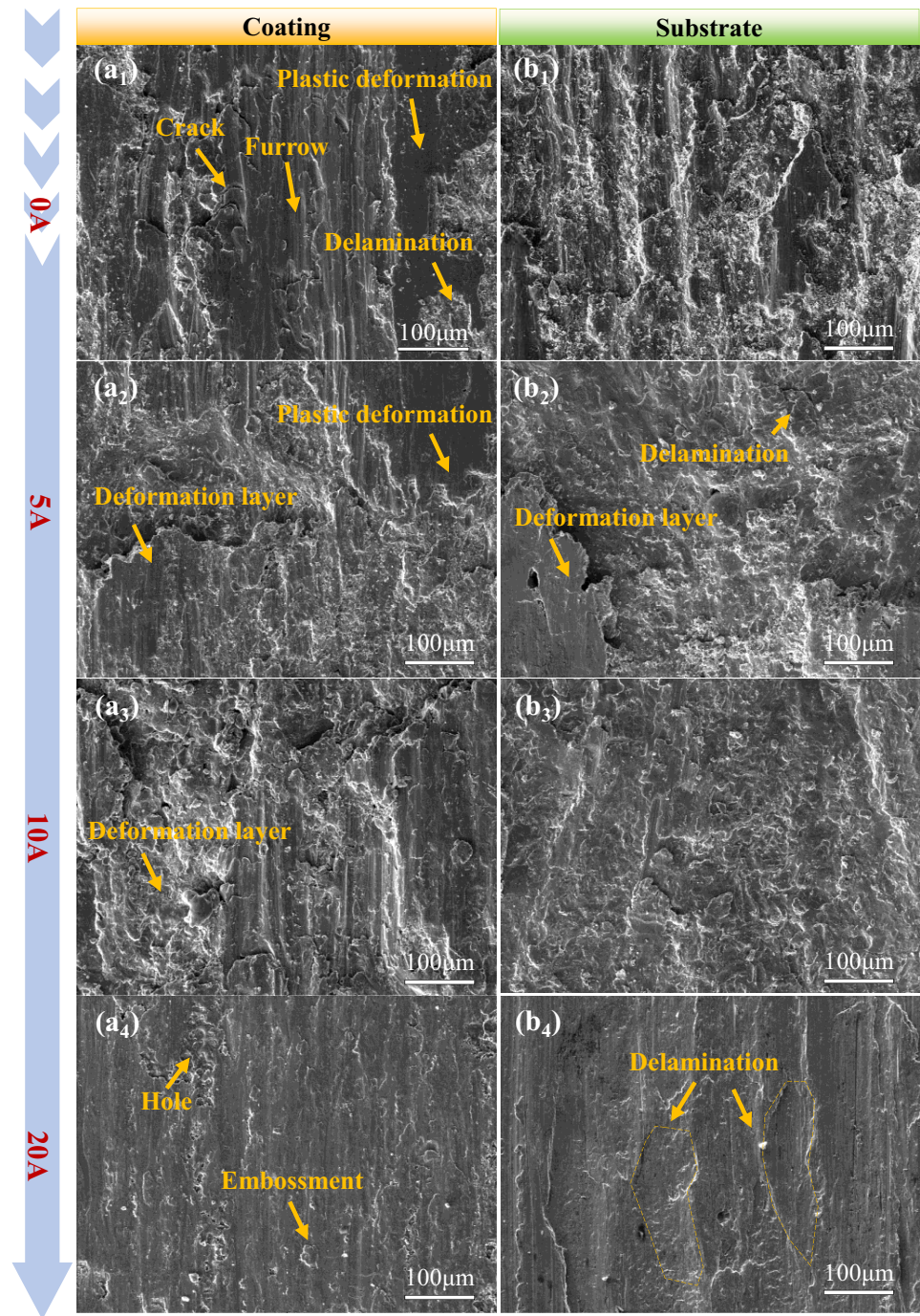
while cracking occurs at the boundaries between hard CrB$_2$ particles and soft Cu matrix by the repeated rotational friction. On the other hand, the QCr0.5 alloy presents a typical morphology of adhesive wear, agreeing well with the low hardness and single-phase structure of QCr0.5 alloy. The plastic deformation and adhesive delamination cause high COF, but there is an additional mechanical battle resulting from CrB$_2$ particles, besides the shear stress caused by plastic bonded interface, resulting in the higher COF of composite coating [30].

With the increase of applied current, the temperature between the friction pairs increases since the Jole heat effect, and then the hardness of the coating and QCr0.5 alloy will decrease. When the value of current is 5A, more serious plastic deformation can be seen,

and some of large deformation layers even cover the worn surface, and the area of furrow decreases but that of the adhesive delamination increases, as shown in Fig. 6a2 and Fig. 6b2. Further increasing the current to 10A, the worn surface presents fully plastic deformation and adhesive delamination, besides some trace of abrasive furrows in the composites coating, seeing in Fig. 6a3 and Fig. 6b3. In this case, the COF will continuously increase due to the serious plastic and adhesive delamination.

However, when the value of current finally increases to 20A, the morphologies of both composite coating and QCr0.5 are totally different from other cases (Fig. 6a4 and Fig. 6b4). There are some squamous embossments and holes on the surface, which may be the result of serious plastic deformation around CrB_2 particles, suggesting the plastic deformation layer of Cu covers the CrB_2 particles or cracking occurs on the CrB_2/Cu interface. At the same time, the heavy plastic deformation suggests the shear resistance of the composite coating is very limited, resulting in the significant decrease in COF at 20A. On the other hand, the area of single delamination increases obviously, which even presents to be "furrow" like, indicating that heavy adhesive wear occurs, which will increase the COF of QCr0.5 sharply.

4 Conclusions

CrB_2/Cu composite coating with 3vol% CrB_2 was prepared on QCr0.5 substrate by laser cladding method, and the current-carrying sliding wear properties are contrastively studied with the QCr0.5 steel. The following conclusions can be drawn:

(1) Most of the CrB_2 particles are retained while some of them decompose into CrB_x phases during the laser cladding process, and then the composite coating consists Cu matrix and irregular CrB_2 and CrB_x particles distributed at the grain boundaries of Cu matrix.

(2) With the increased current value, the COF and wear rate of QCr0.5 alloy increase continuously, but that of CrB_2/Cu coating increases first and then decreases. When the current is 20A, the COF and wear rate of composite coating are about 0.737 and 1.37×10^{-4} mm^3/N•m, which are about 21% and 79% of that of QCr0.5 alloy, respectively.

(3) The increase of both COF and wear rate can be ascribed to the increasing adhesive delamination, since the Jole heat generated by current softens the materials. The abnormal decrease of the COF and wear rate of CrB_2/Cu coating is due to the plastic flow of Cu matrix on CrB_2 particles.

(4) The frictional and wear resistance along with current-passing efficiency CrB_2/Cu coating is better than the commonly used QCr0.5 alloy at 20A, suggesting that the composite coating prepared in this work is suitable for servicing at high current conditions.

Author contributions

Chen Zhang: Methodology, writing—original draft, formal analysis, Data curation; Lei Jia: Funding acquisition, conceptualization, writing—review and editing; Zhen-lin Lu: Supervision, writing—review and editing; Zhi-guo Xing: Writing—review and editing.

Data availability

All data generated or analyzed during this study are included in this published article and we promise that all the original data can be opened if it is necessary and requested.

Declarations

Competing interests   The authors have no competing interests to declare that are relevant to the content of this article.

References

1. A. Najafi, M. Rajabi, Physical properties and microstructural characterization of copper–ZrO$_2$/YSZ nano-composites produced via double-pressing double-sintering method (DPDS). J. Mater. Sci. Mater. Electron. **32**, 28307 (2021)

2. W. Chen, L. Dong, Z. Zhang, H. Gao, Investigation and analysis of arc ablation on WCu electrical contact materials. J. Mater. Sci. Mater. Electron. **27**, 5584 (2016)

3. H. Yang, C. Li, Y. Liu, L. Fu, G. Jiang, X. Cui, B. Hu, K. Wang, Study on the delamination wear and its influence on the conductivity of the carbon contact strip in pantograph-catenary system under high-speed current-carrying condition. Wear **477**, 203823 (2021)

4. Z. Liu, G. Ma, Y. Xiao, T. Yu, H. Wang, W. Guo, Q. Yong, H. Zhao, H. Wang, Microstructure and current-carrying tribological properties of electrobrush-plated Sn-graphene composite coating. J. Mater. Eng. Perform. **32**(1), 29–43 (2023)

5. J. Li, Y. Zhang, C. Song, Y. Sun, T. Chen, Y. Zhang, arc behavior and electrical damage of rolling current–carrying Cu pairs at different rotating speeds. J Mech. Eng. **57**(15), 168–176 (2021)

6. L. Jia, J. Xu, S. Feng Li, Z. Lin Lu, H. Xie, K. Kondoh, Reaction kinetics of Cu–Ni and B$_4$C in Cu–Ni alloy under solid-state sintering. Mater. Sci. Technol. **36**(6), 759–764 (2020)

7. H. Xie, L. Jia, Z. Lu, Microstructure and solidification behavior of Cu–Ni–Si alloys. Mater Charact **60**, 114–118 (2009)

8. Y. Zhu, X.B. Liu, Y.F. Liu, G. Wang, Y. Wang, Y. Meng, J. Liang, Development and characterization of Co-Cu/Ti$_3$SiC$_2$ self-lubricating wear resistant composite coatings on Ti$_6$Al4V alloy by laser cladding. Surf. Coatings Technol. **424**, 127664 (2021)

9. R.P. Chauhan, P. Rana, J. Radioanal, Effect of O5+ ion implantation on the electrical and structural properties of Cu nanowires. Nucl. Chem. **302**, 851 (2014)

10. L. Pawlowski, Suspension and solution thermal spray coatings. Surf. Coatings Technol. **203**, 2807–2829 (2009)

11. L. Ramrakhiani, S. Ghosh, S. Majumdar, Heavy metal recovery from electroplating effluent using adsorption by jute waste-derived biochar for soil amendment and plant micro-fertilizer. Clean Technol. Environ. Policy **24**, 1261–1284 (2022)

12. M. Pellizzari, Z. Zhao, P. Bosetti, M. Perini, Optimizing direct laser metal deposition of H13 cladding on CuBe alloy substrate. Surf. Coatings Technol. **432**, 128084 (2022)

13. Q. Wang, X. Li, W. Niu, X. Rui, X. Mao, Y. Li, J. Yang, Effect of MoS$_2$ content on microstructure and properties of supersonic plasma sprayed Fe-based composite coatings. Surf. Coatings Technol. **391**, 125699 (2020)

14. L. Zhu, P. Xue, Q. Lan, G. Meng, Y. Ren, Z. Yang, P. Xu, Z. Liu, Recent research and development status of laser cladding: a review. Opt. Laser Technol. **138**, 106915 (2021)

15. Q. Xiao, W. Lei Sun, K. Xin Yang, X. Feng Xing, Z. Hao Chen, H. Nan Zhou, J. Lu, Wear mechanisms and micro-evaluation on WC particles investigation of WC-Fe composite coatings fabricated by laser cladding. Surf Coatings Technol **420**, 127341 (2021)

16. B.A. Khamidullin, I.V. Tsivilskiy, A.I. Gorunov, A.K. Gilmutdinov, Modeling of the effect of powder parameters on laser cladding using coaxial nozzle. Surf. Coatings Technol. **364**, 430–443 (2019)

17. Y. Mazaheri, M. Bahiraei, M.M. Jalilvand, S. Ghasemi, A. Heidarpour, Improving mechanical and tribological performances of pure copper matrix surface composites reinforced by Ti$_2$AlCMAX phase and MoS$_2$ nanoparticles. Mater. Chem. Phys. **270**, 124790 (2021)

18. X. Feng Guo, L. Jia, Z. Lin Lu, H. Xie, K. Kondoh, Simultaneous improvement on strength and conductivity of CrB$_2$/Cu composites by inhomogeneous design. Mater. Lett. **349**, 134874 (2023)

19. G. Yao, C. Cao, S. Pan, J. Yuan, I. De Rosa, X. Li, Thermally stable ultrafine grained copper induced by CrB/CrB$_2$ microparticles with surface nanofeatures via regular casting. J. Mater. Sci. Technol. **58**, 55–62 (2020)

20. X. Feng Guo, L. Jia, Z. Lin Lu, Z. Guo Xing, H. Xie, K. Kondoh, Preparation of Cu/CrB$_2$ composites with well-balanced mechanical properties and electrical conductivity by ex-situ powder metallurgy. J. Mater. Res. Technol. **17**, 1605–1615 (2022)

21. C. Zhang, L. Jia, Z. Lu, Z. Xing, Statistical modeling and optimization on laser cladding craft for preparing CrB$_2$/Cu coating on copper substrate. J. Mater. Eng. Perform. **33**, 4538–4551 (2024)

22. J. Hao, F. Hu, X. Le, H. Liu, H. Yang, J. Han, Microstructure and high-temperature wear behaviour of Inconel 625 multi-layer cladding prepared on H13 mould steel by a hybrid additive manufacturing method. J. Mater. Process. Tech. **291**, 117036 (2021)

23. O.A. Tertuliano, P.J. Depond, D. Doan, M.J. Matthews, X.W. Gu, W. Cai, A.J. Lew, Nanoparticle-enhanced absorptivity of copper during laser powder bed fusion. Addit. Manuf. **51**, 102562 (2022)

24. G. Wang, X.-B. Liu, G.-X. Zhu, Y. Zhu, Y. Liu, L. Zhang, J. Wang, Tribological study of Ti$_3$SiC$_2$/Cu$_5$Si/TiC reinforced

co-based coatings on sus304 steel by laser cladding. Surf. Coatings Technol. **432**, 128064 (2022)

25. G. Mei, Impact of voltage on the electric sliding tribological properties of current collectors against overhead lines. Wear **474**, 203868 (2021)

26. Q. Chai, C. Fang, X. Qiu, Y. Xing, G. Sun, Modeling of temperature field and profile of Ni60AA formed on cylindrical 316 stainless steel by laser cladding. Surf. Coatings Technol. **428**, 127865 (2021)

27. Y. Wei Wang, X. Wen Sun, L. Wang, Y. Yang, X. Xing Ren, Y. Duo Ma, Y. Hang Cui, W. Wei Sun, X. Yu Wang, Y. Chun Dong, Microstructure and properties of CrB_2-Cr_3C_2 composite coatings prepared by plasma spraying. Surf Coatings Technol **425**, 127693 (2021)

28. G. Yao, J. Yuan, S. Pan, Z. Guan, C. Cao, X. Li, Casting in-situ Cu / CrB_x composites via aluminum-assisted reduction. Procedia Manuf. **48**, 320–324 (2020)

29. S. Wen, P. Huang, Principles of tribology, second ed. Tsinghua University Press, Bei Jing, 282–283 (2002) (In chinese)

30. S. Zhang, H. Kang, M. Cheng, Y. Jiang, F. Cao, E. Guo, Z. Chen, S. Liang, T. Wang, A research on the electrical sliding behavior wear of dual-scale particulate reinforced copper matrix composites. Mater Charact **184**, 111708 (2022)